Title

Tensile nanomechanics and the Hall-Petch effect in nanocrystalline aluminium

Authors

Xu, Wenwu

Dávila, Lilian P

Publication Date

2018

DOI

10.1016/j.msea.2017.10.021

Peer reviewed

Materials Science & Engineering A 710 (2018) 413–418

Contents lists available at ScienceDirect

Materials Science & Engineering A

journal homepage: www.elsevier.com/locate/msea

Tensile nanomechanics and the Hall-Petch effect in nanocrystalline aluminium

Wenwu Xu[a,b], Lilian P. Dávila[a,*]

[a] Materials Science and Engineering, School of Engineering, University of California Merced, 5200N. Lake Road, Merced, CA 95343, USA
[b] Mechanical Engineering, School of Engineering, San Diego State University, 5500 Campanile Drive, San Diego, CA 92182, USA

ARTICLE INFO

Keywords:
Nanocrystalline
Hall-Petch effect
Molecular dynamics
Size dependence
Aluminum

ABSTRACT

This work carries out comprehensive classical molecular dynamics simulations of uniaxial tensile deformation for nanocrystalline Al samples with a broad range of different mean grain sizes. The largest nanocrystalline Al sample has a mean grain size of about 30 nm and contains over 100 millions atoms in the modeling system. The grain size dependence of yield stress and the atomic fraction of dislocations are quantified and the size dependence tensile nanomechanics are also revealed. Deformation twinning and grain boundary migration are observed as main mechanisms of tensile deformation in the nanocrystalline Al. In particular, the complete Hall-Petch relationship for the nanocrystalline Al bulk is determined for the first time in this study, from which three distinct regions are identified including the normal, inverse, and extended regions in the Hall-Petch relationship. We expect these findings will provide useful insights in the nanomechanics of nanocrystalline Al. The quantitation analyses on dislocations and mechanical properties may facilitate the design and development of high strength nanocrystalline Al and Al based alloys as well as future testing procedures for promising structural and transportation applications.

1. Introduction

Nanocrystalline metals and alloys show characteristic mechanical properties different from those of conventional coarse-grained polycrystalline counterparts attributed to their large volume fraction of interfaces, e.g. grain boundaries, phase boundaries, and domain interfaces [1–3]. For instance, grain boundary strengthening (or Hall-Petch (HP) relationship [4,5]) is a known mechanism of strengthening materials by altering their average grain sizes (equivalent to changing the volume fraction of grain boundaries). As the grain size reduces from microscale to nanoscale, the yield stress or hardness increases (with a positive slope in the HP relationship) and then decreases (with a negative slope in the HP relationship). As a consequence, a maximum threshold value of yield stress or hardness is generally reached at certain grain size level for a given nanocrystalline metal or alloy. Numerous reports show that the transition of positive to negative slope in the HP relationship is around 10–40 nm for varied nanocrystalline metals and alloys [6–8], such as Al [9–11], Fe [12], Cu [6,13,14], Cu-Ta [15], Ni [6], Ni-P [13], Zr [16], and Zn [17] among others.

In general, grain boundaries (and twin boundaries in some cases, such as in the nanocrystalline Al [18,19] and Cu [14,15] systems) and dislocation motion play an important role in elastic and plastic deformation processes, which are crucial factors in controlling the mechanical properties of nanocrystalline metals, particularly at the nanoscale [18–20]. Below certain grain sizes, most of the dislocation generation and storage takes place at the grain boundary regions as opposed to the larger grain interior regions [15]. In addition, with the reduction of grain size from microscale to nanoscale, the dislocation motion becomes strongly size dependent and both dynamic recovery and annihilation of dislocations increase [15], which ultimately limits the capacity for dislocation storage at fine-grained nanocrystalline metals.

Aluminum (and its alloys) is among the most widely used lightweight metals with continuing applications to meet societal challenges of high performance structures and energy efficient transportation systems. In this work, we investigate the nanomechanics with atomic level detail of nanocrystalline pure metal Al using molecular dynamics (MD) simulations to carry out the quantification analysis of dislocations as a function of mean grain size during tensile deformation. Additionally, the comprehensive HP relationship (yield stress vs. mean grain size) is evaluated for the nanocrystalline Al bulk. Understanding how size dependence influences grain boundaries and dislocations on the deformation process and mechanical properties of this material system will provide important fundamental details and significant

* Corresponding author.
E-mail address: ldavila@ucmerced.edu (L.P. Dávila).

http://dx.doi.org/10.1016/j.msea.2017.10.021
Received 25 June 2017; Received in revised form 3 October 2017; Accepted 4 October 2017
Available online 07 October 2017
0921-5093/

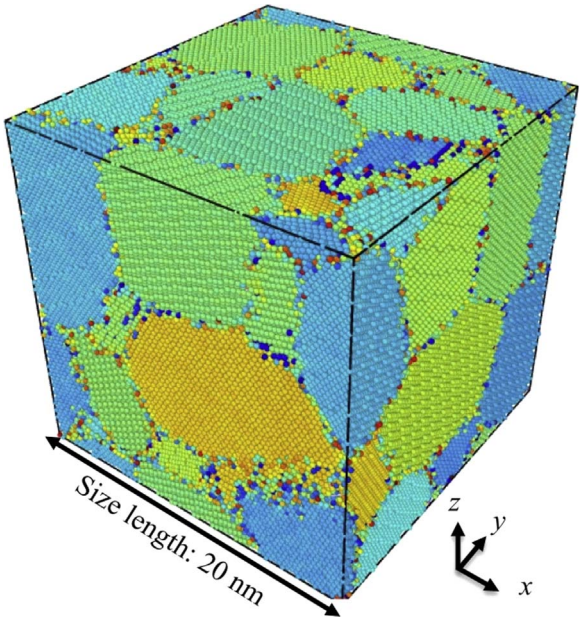

Fig. 1. Representative nanocrystalline Al bulk model (cubic with side length of 20 nm) with a mean grain size (d) of 4.4 nm containing 20 grains and over 1.6 million atoms. The grain crystal orientations and boundaries are differentiated by colors. (For interpretation of the references to color in this figure legend, the reader is referred to the web version of this article.)

guidance to develop advanced nanocrystalline metals and alloys with tunable mechanical properties.

2. Molecular dynamics simulation and analysis

2.1. Model creation of nanocrystalline Al

Fourteen atomistic models of nanocrystalline Al bulk structures are created with different mean grain sizes ranging from 1.1 to 29.6 nm using a Voronoi construction method [21]. Each nanocrystalline model consists of 20 grains with a lognormal size distribution. The number of 20 grains per nanocrystalline model is specifically chosen to ensure that realistic polycrystalline plastic flow during deformation would be observed. As the mean grain size increases, the nanocrystalline sample increases both in the number of atoms in the model from 7.31×10^3 to 1.04×10^8 and the side lengths of the cubic model from 5 nm to 120 nm. Fig. 1 shows a representative nanocrystalline Al cubic model with a side length of 20 nm and a mean grain size (d) of 4.4 nm (1.6×10^6 atoms). The color of atoms in Fig. 1 indicates the local structural environment (per atom), computed by using the polyhedral template matching (PTM) [22] method that is implemented in the OVITO software [23]. The PTM approach offers greater reliability than the common neighbor analysis (CNA) in the case of high strains [22]. PTM provides an atomic mapping of local orientation (per atom), from which various crystalline defects such as grain boundaries (GBs), twin boundaries, and dislocations can be readily identified (as shown via distinct colors in Fig. 1) that can expand analysis further.

In this study, MD simulations are performed using the Large-scale Atomic/Molecular Massively Parallel Simulator (LAMMPS) open-source code [24]. For the MD modeling, we use the embedded atom method (EAM) potential developed by Mishin et al. [25] established on the basis of experimental data and *ab initio* calculations. All of the nanocrystalline Al models are relaxed to equilibrium configurations at 300 K with a pressure of 0 bar by using a Nose/Hoover type equation of motion sampled from isothermal-isobaric (NPT) ensemble. Simulation times of 50–100 ps (i.e. 50,000–100,000 steps with a time step of 0.001 ps) are found to be adequate for such relaxations. Periodic boundary conditions (PBC) are also employed in the nanocrystalline models. All the nanocrystalline Al models in this study are in agreement with experimental observations (e.g. TEM characterization) regarding grain morphology of nanocrystalline materials with varied mean grain sizes [1].

2.2. Uniaxial tensile deformation

MD simulations of uniaxial tension deformation along x- axis (see Fig. 1) are carried out for the 14 different nanocrystalline Al models. Periodic boundary conditions are used. The uniaxial tension load is simulated by changing the length of the nanostructured model along the x- axis. For each nanocrystalline sample, a uniform strain field along the required direction is accomplished by repeatedly scaling the corresponding unit cell and the atomic positions by a factor of 1.01 of the initial coordinates, and then relaxing the model for 50 ps in between rescaling steps. This tensile/relaxation step is repeated until a strain of 0.5 was reached. The tensile strain here is the engineering strain, that is, $\varepsilon = \Delta L/L_0$, where ΔL is the change relative to the original length L_0. In this study, a strain rate of $10^{10}\ s^{-1}$ is applied to all 14 nanocrystalline models to investigate the nanograin size effect on the tensile nanomechanics and the Hall-Petch relationship of nanocrytalline Al. During deformation, the lateral boundaries of each sample are kept constant at zero pressure. This tensile method is comparable to techniques reported previously in the study of silica nanowires [26], metallic nanowires [27] and nanocrystalline bulk [28]. The effect of mean grain size (d) on dislocation formation and the Hall-Petch relationship (e.g. yield stress) were analyzed and point defects were subsequently quantified.

3. Results and discussion

3.1. Tensile nanomechanics and point defect evolution

The tensile behavior is analyzed for all nanocrystalline Al models using stress-strain curves. The simulated tensile behavior is similar in all 14 models with a linear increase in stress-strain curves prior to reaching the ultimate tensile strength, yet with different slopes up to yield levels in different nanocrystalline models as previously reported [28]. Structural analysis was also performed in all 14 simulated nanocrystalline Al models using similar techniques as before [28].

Fig. 2 shows successive snapshots of the atomic structure evolution during uniaxial tensile deformation as strain (ε) increases in a nanocrystalline Al bulk model (mean grain size d of ~ 4.4 nm), i.e. (a) $\varepsilon = 0$, (b) $\varepsilon = 0.1$, (c) $\varepsilon = 0.2$, (d) $\varepsilon = 0.3$, and (e) $\varepsilon = 0.4$. As shown via Supplementary Animation I the full tensile deformation simulation of a nanocrystalline Al bulk sample with mean grain size of 4.4 nm can be observed. Fig. 2(a) presents a 2D view of x-z plane of the original unstrained nanocrystalline model shown in Fig. 1 ($\varepsilon = 0$). Moreover, the atomic evolution during the initial stage of elastic tensile deformation ($\varepsilon < 0.02 \sim 0.05$) in this bulk model is further analyzed (see Supplementary Fig. S1 and Animation II). As the deformation process develops, from elastic ($\varepsilon < 0.02 \sim 0.05$) to plastic region ($\varepsilon > 0.02 \sim 0.05$), a variety of intra- and inter-granular atomic mobilities of point defects, dislocations and GBs, are identified in the nanocrystalline Al bulk with varied mean grain sizes.

As shown via Supplementary Fig. S1 and Animation II, in the case of tensile deformation of a nanocrystalline Al bulk model with grain size of 4.4 nm, one observes distinct traits. At the elastic deformation region ($\varepsilon < 0.02 \sim 0.05$) where stress is below the formation of dislocations, the coordination numbers of atoms at random lattice sites (shown with light blue color, a number of such atoms are highlighted via white arrows in Fig. S1) in the grain interiors deviate slightly from that of the perfect face-centered cubic (FCC) crystal structure of Al (shown with dark blue color in Fig. S1). This is due to the subtle lattice distortion resulted from the small elastic strain. It is noteworthy that these lattice

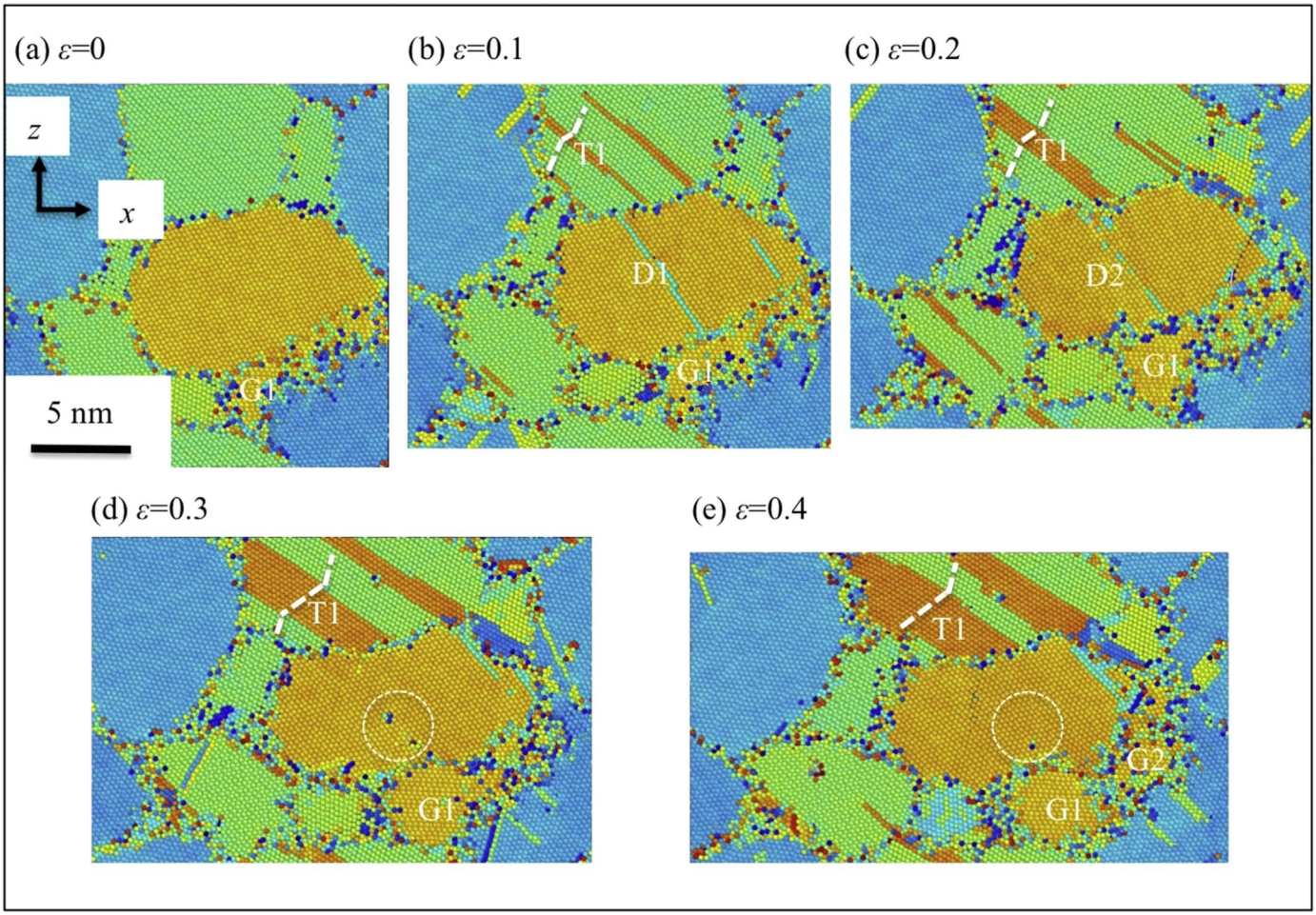

Fig. 2. Typical atomic displacements during uniaxial tensile deformation of a nanocrystalline Al bulk (mean grain size *d* of 4.4 nm) with increasing strain (ε). The local structural environment (per atom) is distinguished by colors. T1 indicates twin structures guided by the white zigzag dashed lines. D1 and D2 show the formation and dissolving of a stacking fault, respectively. G1 and G2 represent the growth of a grain and the new formation of a grain due to the GB migrations. Other point defects are shown as white dashed circles. (For interpretation of the references to color in this figure legend, the reader is referred to the web version of this article.)

point defects either annihilate or tend to move to GB regions with increasing elastic strain. The ideal FCC coordination numbers of atoms in the grain interior regions are therefore sustained during the initial elastic deformation region. The significantly smaller distance of adjacent GBs in the nanocrystalline Al bulk as compared with its conventional coarse-grained polycrystalline system allows a shorter path of transportation of these lattice point defects towards GB regions. As a result, the elasticity of the nanocrystalline Al bulk may likely increase, especially when the grain size is less than a few nanometers. This is consistent with the observation of elastic modulus as a function of grain size in the nanocrystalline Al samples (see Fig. 4(a) in the Ref. [28]). The significant (exponentially) decrease in elastic (Young's) modulus represents apparent increase in the elasticity, thus the obvious increase of elastic region or elastic strain under tensile load is observed.

As strain reaches certain levels ($\varepsilon = 0.02 \sim 0.05$ for various nanocrystalline Al with different mean grain sizes), all dislocations begin to nucleate simultaneously at the GB regions (see Supplementary Fig. S1, part (f)) and no dislocation is found to form in the grain interior regions of the nanocrystalline Al with a mean grain size (*d*) of 4.4 nm. Then, with further increases of strain ($\varepsilon > 0.02 \sim 0.05$), some dislocations are able to move across the entire grain along certain lattice planes reaching another side of the GB region and then disappear or sink at the GB region (see Fig. 2). This type of dislocation process has a number of consequences as delineated below.

Firstly, during the movement of these dislocations (Fig. 2) the associated atoms move a very small distance relative to their neighbors along the same direction as that for the movement of dislocation, causing the formation of twinning structures (e.g. labeled as T1 with zigzag white dashed lines in Fig. 2(b)). These atomic-scale twins can grow in width (up to nanometer-scale) if multiple events of dislocation movement across the entire grain happen continuously in the adjacent crystal lattice planes (e.g. orange colored twin, labeled T1 in Fig. 2, parts (c)-(e)). The increase of twin width may halt as it expands to the GB region (see Fig. 2(e)). Twinning thus becomes a preferred deformation mechanism in Al with a grain size of a few nanometers. This is consistent with high-resolution transmission electron microscope (HRTEM) observations [19]. The presence of grown-in twins in nanocrystalline Al may also enhance plastic deformation via twin-migration in which partial dislocations, emitted at the intersection of the twin boundary and the GB, travel through the entire grain [29].

Secondly, if only a single (non-continuously) event of dislocation movement across the entire grain occurs the dislocation may eventually 'sink' at the GB region during the tensile deformation. The sink of dislocation at the GB region has been considered as one of the most important deformation mechanisms in nanocrystalline metals [20]. Interestingly, the movement of this type of dislocation may leave behind stacking fault transecting the grain [18] followed by its 'dissolving' in the grain interior region (denoted as D1 and D2 in Fig. 2, parts (b)–(c)). Therefore, a number of point defects are formed and these point defects tend to agglomerate and move toward the GB region (see defects within the white dashed circles in Fig. 2, parts (d)–(e)). Both the sinking and dissolving of dislocation do not maintain additional crystal

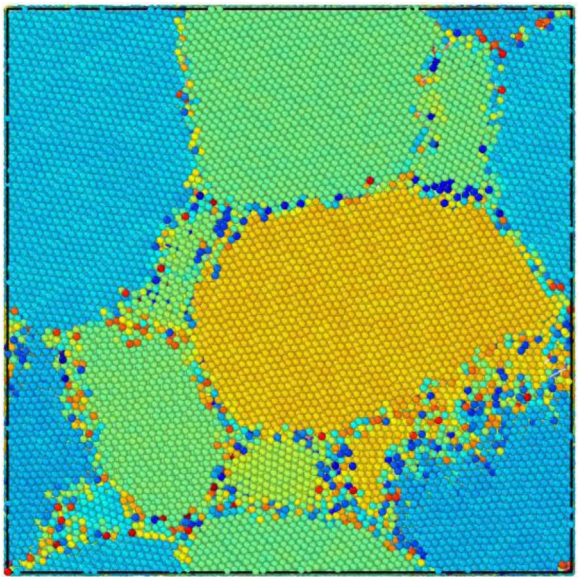

Video S1. Atomic structure evolution during uniaxial tensile deformation with the increase of strain in a nanocrystalline Al bulk (mean grain size about 4.4 nm) at a strain rate of 10^{10} s^{-1}. The grain crystal orientation and grain boundaries are distinguished by colors. Supplementary material related to this article can be found online at http://dx.doi.org/%2010.1016/j.msea.2017.10.021.

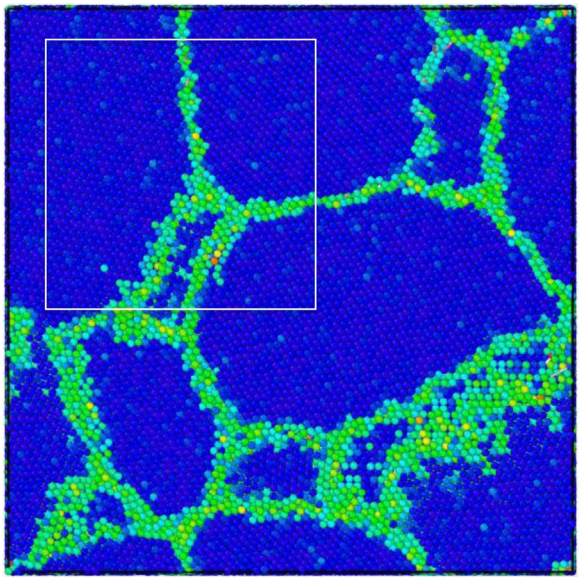

Video S2. Atomic structure evolution during uniaxial tensile deformation with the increase of strain in a nanocrystalline Al bulk (mean grain size about 4.4 nm) at a strain rate of 10^{10} s^{-1}. Atoms are colored according to local structural environment. Blue atoms possess perfect FCC structure. Green or yellow atoms are of non-FCC or disordered atomic arrangements. Note the consecutive snapshots of the initial elastic process ($0.01 \leq \varepsilon \leq 0.06$) of the region within the white solid square is shown in Figure S1. Supplementary material related to this article can be found online at http://dx.doi.org/%2010.1016/j.msea.2017.10.021.

lattice defects in the grain interior region during tensile deformation. The perfect FCC crystal structure in the grain interior region is thus maintained (unchanged) during deformation, which benefits via the enhancement of tensile strength of the nanocrystalline Al bulk. It should be noted that due to an inherent limitation of MD simulations, the high deformation rate applied in simulations may induce rather high stresses that are usually much larger than results of experiments. In addition, the strain rate of 10^{10} s^{-1} used in our simulations may also be in the range of plasticity controlled by dislocation nucleation that is sourced at grain boundaries in nanocrystalline materials.

Lastly, the generation of twin interfaces and stacking faults offers an alternative path to dislocation pile-up at grain boundaries to explain the continuous grain-size strengthening and the strain hardening of nanocrystalline materials [19]. As shown above, our simulations illustrate the manner in which dislocation-based deformation of nanocrytalline Al differs substantially from the well-studied behaviors of conventional coarse-grained polycrystalline materials. Additionally, we observe GB migration during the tensile deformation process. This deformation mechanism is often reported in nanocrystalline material systems, especially when the mean grain size is only a few nanometers [1]. The migration of GBs is due to the GB defect migration achieved by emitting dislocations. It may cause grain growth (marked as G1 in Fig. 2, parts (b)–(e)) or the formation of new grains (shown as G2 in Fig. 2, part (e)). The origin of this can be explained, as the grain size decreases down to a few nanometers, the nucleation of complete dislocations is no longer possible, and the dislocation-slip mechanics ceases to be operational, in favor of a GB-based deformation mechanics [20]. GB migration associated new grain formation and growth has also been observed in previous work [29].

3.2. Quantification of dislocations

It is generally agreed that the atomic arrangement of dislocation in FCC Al is of hexagonal close packing (HCP) stacking sequence. In addition, no FCC to HCP structure transformation in nanocrystalline Al has ever been discovered. It is then reasonable to believe that the atomic fraction of HCP stacking atoms is approximately the same as the atomic fraction of HCP stacking dislocations in FCC Al. This is computed via the PTM calculations described earlier (see Section 2.1). Fig. 3 summarizes the quantification analysis of dislocations in several nanocrystalline Al bulk models with different mean grain sizes. As shown in Fig. 3(a), the atomic fraction of dislocation (X_D) depends on both the strain (ε) and the mean grain size (d). For each case at different mean grain sizes, the atomic fraction of dislocations (X_D) remains essentially at zero when $\varepsilon < 0.02 \sim 0.05$, undergoes an abrupt increase in the range of $0.05 < \varepsilon < 0.10$, and eventually reaches a relatively high level that is maintained with further increase of strain.

Interestingly, the high level of atomic fraction of dislocations (X_D) increases as the mean grain size (d) increases as well in the nanocrystalline Al bulk models, showing a significant size-dependence. Further analysis led to the correlation of maximum value of the atomic fraction of dislocations ($X_D{}^M$) with the mean grain size in the nanocrystalline Al bulk under tensile deformation. Fig. 3(b) shows that the atomic fraction of dislocations ($X_D{}^M$) reaches increasingly higher level with the increase of mean grain size (d). In fact, this behavior follows a non-linear relationship that can be approximated by a power law function: $X_D{}^M = 0.02d^{0.2}$ (as indicated by the red solid curve in Fig. 3(b)), where d is the mean grain size. This is probably because finer grained Al bulk samples allow fewer formation and movement of dislocations simultaneously. The quantification analysis of size dependence dislocation behavior may provide useful in-sights toward understanding the role of grain size on the mechanical properties of nanocrystalline bulk systems, for example, the Hall-Petch strengthening [4,5] – a method of strengthening materials by modifying their mean grain size.

3.3. Hall-Petch relationship of nanocrystalline Al bulk models

By atomistic simulating uniaxial tensile deformation (see Section 2.2), we obtain the stress-strain curves of 14 different nanocrystalline Al bulk models with mean grain size ranging from 1.1 to 29.6 nm at a strain rate of 10^{10} s^{-1}. Representative stress-strain curves have previously been reported [28]. We subsequently compute the yield stress (i.e. stress corresponding to the linear limit of the stress-strain curve)

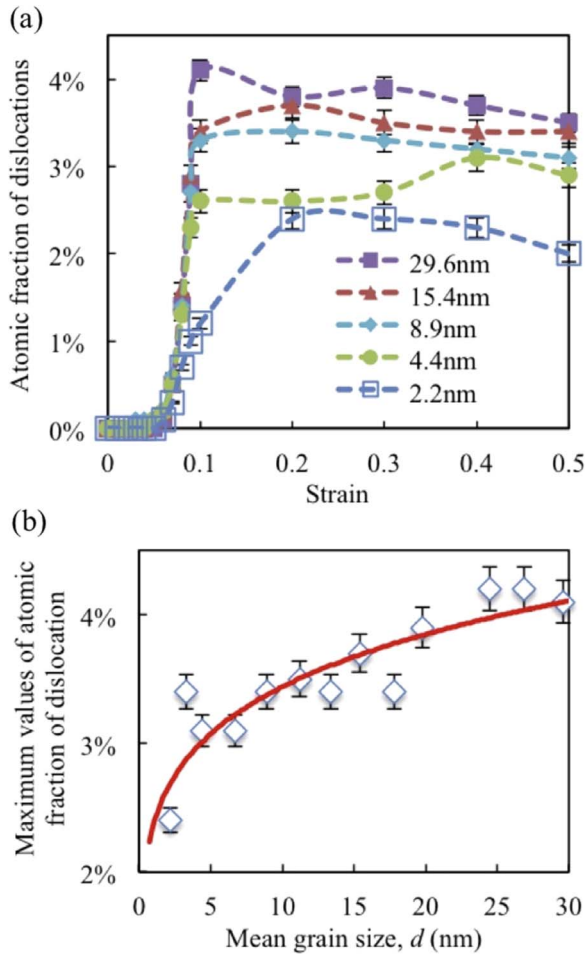

Fig. 3. Quantification of dislocations in different nanocrystalline Al bulk models during tensile deformation shows distinct behaviors: (a) atomic fraction of dislocations (X_D) as a function of strain (ε) for varied mean grain sizes (d); (b) maximum values of atomic fraction of dislocations (X_D^M) as a function of d (fitted by a power law function: $X_D^M = 0.02d^{0.2}$, 1.1 nm $\leq d \leq$ 29.9 nm) for the nanocrystalline Al bulk models.

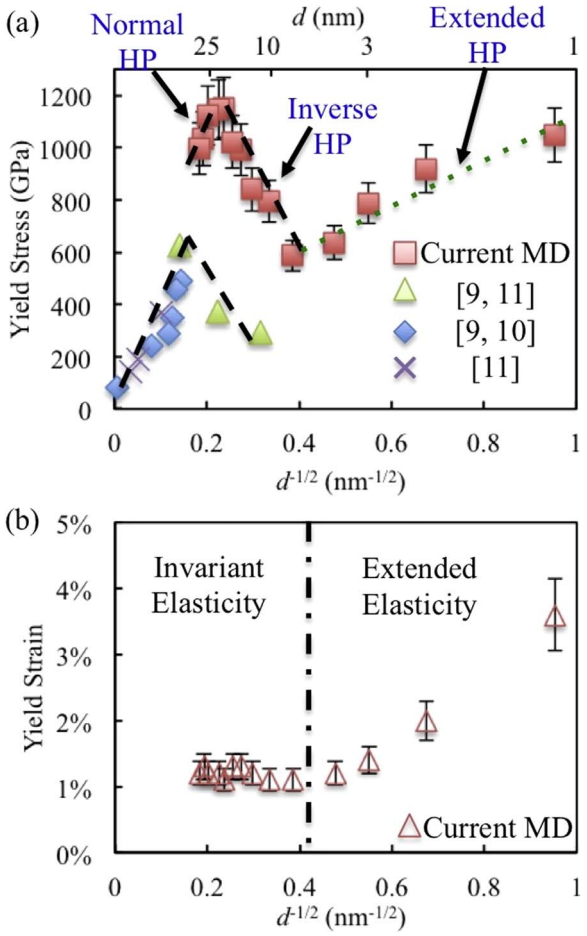

Fig. 4. Hall-Petch (HP) relationship for the nanocrystalline Al bulk cases: (a) size dependence of yield stress in this MD study is indicated by red closed squares with associated error bars at a strain rate of $10^{10}\,s^{-1}$. Prior experimental measurements are also included for comparison purposes (strain rate about $10^{-4}\,s^{-1}$). Part (b) shows size dependence of yield strain reported in this study only, which reveals varied elasticity phenomena that can explain the origin of the extended HP region for this material system. (For interpretation of the references to color in this figure legend, the reader is referred to the web version of this article.)

for each nanocrystalline Al bulk. The resulting size dependent yield stress calculations (in this study and previous studies) are summarized in Fig. 4(a). MD findings from the present study are represented by red closed squares with associated error bars. This is the so-called Hall-Petch (HP) relationship of nanocrystalline Al bulk samples at a strain rate of $10^{10}\,s^{-1}$.

Most interestingly, we observe three distinct regions in the HP relationship depicted in Fig. 4(a) marked as: normal, inverse, and extended HP regions, with trends highlighted by black dashed and green dotted lines, respectively. The **normal** region of the HP relationship corresponds to the classical HP description (with a positive slope in the HP relationship) [4,5], from which one would expect an increase in the yield stress (strength) of microcrystalline bulk materials with relatively small grain size. This behavior is attributed to the pile-ups in fine-grained materials containing fewer dislocations, with the stress at the tip of the pile-up decreasing and, thus a larger applied stress is required to generate extra dislocations in adjacent grains [6].

As the mean grain size (d) reduces further in the nanocrystalline Al bulk models, the normal HP relationship breaks down because grains are unable to support further dislocation pile-ups [6] since the equilibrium distance between dislocations exceeds the grain size. As a result, a threshold value is expected at which a maximum yield stress can be achieved. This threshold value is found to be about 25 nm in the case of nanocrystalline Al bulk as shown in Fig. 4(a). Beyond this threshold, the slope of the HP relationship becomes negative, i.e. the yield stress decreases with further decreasing of mean grain size. This is known as the **inverse** HP effect [30], also shown in Fig. 4(a).

Reported experimental measurements of the yield stress at a strain rate of $10^{-4}\,s^{-1}$ of microcrystalline and nanocrystalline Al samples with different mean grain sizes are included for comparison in Fig. 4(a) [9–11]. Two distinct regions of normal and inverse HP relationships (shown as black dashed lines) are observed, from which a threshold value of about 30 nm is identified. It is also observed that the slopes of the normal and inverse HP relationships in Fig. 4(a) agree very well when comparing experimental measurements and the current MD simulations. The difference or "shift" in yield stress values between experiments and our MD study is due to the strain rate sensitivity of the Hall-Petch relationship – where a high strain rate usually results in high yield stresses [7,31]. The intrinsic characteristic of simulation time step (on the order of femtoseconds) in atomic scale approaches limits the strain rate that can be achieved (i.e. MD simulation generally shows a few orders of magnitudes greater strain rates than in experiments). In addition, the experimental threshold value (i.e. 30 nm), at which the maximum yield strength of nanocrytalline Al bulk is reached, agrees reasonably well with that from the current MD simulation (i.e. 25 nm). The deviation between experiments and MD simulation is likely due to the existence of defects (e.g. nanoscale pores) in the experimental samples produced by various fabrication techniques and processing.

Additionally, we notice that at a particular ultrafine nanograin size

($d < \sim 5$ nm or $d^{-1/2} \sim 0.4\,\mathrm{nm}^{-1/2}$) as seen in Fig. 4(a), a new "extended" HP relationship emerges in our MD results – in which the yield stress increases again with further decreasing of mean grain size. This is a direct consequence of the increased elasticity (i.e. linear limit in the stress-strain curve) in the nanocrystalline Al bulk models with ultrafine nanograin size. As previously reported in our work [28], we noticed that there is a significant (exponentially) decrease in elastic (Young's) modulus when the mean grain size in nanocrystalline Al samples is less than around 10 nm. This indicates an apparent increase in the elasticity, thus the obvious increase of elastic region or yield strain under tensile loading can be observed in the ultrafine nanocrystalline materials.

The MD calculated yield strains (i.e. corresponding to yield stresses in Fig. 4(a)) for each of the nanocrystalline Al bulk models with different mean grain sizes are shown in Fig. 4(b). It is observed that the elastic strain limit maintains the same value when the mean grain size is reduced to about 5 nm (or $d^{-1/2} \sim 0.4\,\mathrm{nm}^{-1/2}$), and then increases rapidly with further decrease of mean grain size (d). Thus, the increased elastic strain limit leads to an increased yield stress in the nanocrystalline Al bulk cases with ultrafine mean grain sizes. This is because in the ultrafine-grained nanocrystalline Al models ($d < \sim 5$ nm) there are over 10–50% of atoms located at the GB regions and possess disordered arrangements [28]. These disordered GBs become great 'buffer layers' for the sink of point defects created during the elastic deformation process (see Supplementary Fig. S1). Consequently, the perfect FCC crystal structure in the grain interiors is maintained at a relatively larger elastic deformation, and the elastic region (or limit) of ultrafine-grained nanocrystalline Al is further increased, giving rise to the **extended** HP effect.

4. Conclusions

This work investigated comprehensively the grain size dependence of the tensile deformation and mechanical properties in different nanocrystalline Al bulk models using large-scale molecular dynamics simulations. The deformation twinning and grain boundary migration were analyzed and found to be important deformation mechanisms, particularly when the mean grain size is on the order of a few nanometers. The calculation of atomic fraction of dislocations due to the tensile deformation in the nanocrystalline Al bulk reached different levels depending on the grain sizes. Most significantly, the complete Hall-Petch relationship for fourteen nanocrystalline Al bulk models was simulated, from which three distinct regions were quantified and evaluated including the normal, inverse, and extended regions in the Hall-Petch relationship. We expect these findings will provide useful insights in the nanomechanics of nanocrystalline Al samples and the quantitation analyses on dislocations and mechanical properties can facilitate the design and development of high strength nanocrystalline Al and Al based alloys for promising structural and transportation applications.

Acknowledgements

This work was performed under the auspices of an internal grant at the University of California, Merced. The authors also wish to thank the Triton Shared Computing Cluster (TSCC) at San Diego Supercomputer Center (SDSC) for providing computing support for this project.

Appendix A. Supplementary information

Supplementary data associated with this article can be found in the online version at doi:10.1016/j.msea.2017.10.021

References

[1] H. Gleiter, Nanostructured materials: basic consepts and microstructure, Acta Mater. 48 (2000) 1–29.
[2] W. Xu, X. Song, N. Lu, C. Huang, Thermodynamic and experimental study on phase stability in nanocrystalline alloys, Acta Mater. 58 (2010) 396–407.
[3] K.A. Darling, M. Rajagopalan, M. Komarasamy, M.A. Bhatia, B.C. Hornbuckle, R.S. Mishra, K.N. Solanki, Extreme creep resistance in a microstructurally stable nanocrystalline alloy, Nature 537 (2016) 378–381.
[4] N.J. Petch, The cleavage strength of polycrytals, J. Iron Steel Ins. 174 (1953) 25–28.
[5] E.O. Hall, The deformation and ageing of mild steel: iii discussion of results, Proc. Phys. Soc. Lond. Sec. B 64 (1951) 747–753.
[6] C.E. Carlton, P.J. Ferreira, What is behind the inverse Hall-Petch effect in nanocrystalline materials? Acta Mater. 55 (2007) 3749–3756.
[7] K.S. Kumar, H. Van Swygenhoven, S. Suresh, Mechanical behavior of nanocrystalline metals and alloys, Acta Mater. 51 (2003) 5743–5774.
[8] H. Van Swygenhoven, J.R. Weertman, Deformation in nanocrystalline metals, Mater. Today 9 (2006) 24–31.
[9] H.J. Choi, S.W. Lee, J.S. Park, D.H. Bae, Tensile behavior of bulk nanocrystalline aluminum synthesized by hot extrusion of ball-milled powders, Scr. Mater. 59 (2008) 1123–1126.
[10] H.J. Choi, S.W. Lee, J.S. Park, D.H. Bae, Positive deviation from a Hall-Petch relation in nanocrystalline aluminum, Mater. Trans. 50 (2009) 640–643.
[11] G. Jeong, J. Park, S. Nam, S.-E. Shin, J. Shin, D. Bae, H. Choi, The effect of grain size on the mechanical properties of aluminum, Arch. Metall. Mater. 60 (2015) 1287–1291.
[12] J. Jeon, B. Lee, W. Chang, Molecular dynamics simulation study of the effect of grain size on the deformation behavior of nanocrystalliine body-centered cubic iron, Scr. Mater. 64 (2011) 494–497.
[13] C.S. Pande, K.P. Cooper, Nanomechanics of Hall–Petch relationship in nanocrystalline materials, Prog. Mater. Sci. 54 (2009) 689–706.
[14] J. Schiotz, K.W. Jacobsen, A maximum in the strength of nanocrystalline copper, Science 301 (2003) 1357–1358.
[15] M.A. Tschopp, H.A. Murdoch, L.J. Kecskes, K.A. Darling, "Bulk" nanocrystalline metals: review of the current state of the art and future opportunities for copper and copper alloys, JOM 66 (2014) 1000–1019.
[16] B. Wang, V. Tomar, A. Haque, In-situ TEM mechanical testing of nanocrystalline zirconium thin films, Mater. Lett. 152 (2015) 105–108.
[17] D. Wolf, V. Yamakov, S.R. Phillpot, A. Mukherjee, H. Gleiter, Deformation of nanocrystalline materials by molecular-dynamics simulation: relationship to experiments? Acta Mater. 53 (2005) 1–40.
[18] V. Yamakov, D. Woft, S.R. Phillpot, A.K. Mrkherjee, H. Gleiter, Deformation-mechanism map for nanocrystalline metals by molecular dynamics simulation, Nat. Mater. 3 (2004) 43–47.
[19] M. Chen, E. Ma, K.J. Hemker, H. Sheng, Y. Wang, X. Cheng, Deformation twinning in nanocrystalline aluminum, Science 300 (2003) 1275.
[20] V. Yamakov, D. Wolf, S.R. Phillpot, A.K. Kukherjee, H. Gleiter, Dislocation processes in the deformation of nanocrystalline aluminum by molecular-dynamics simulation, Nat. Mater. 1 (2002) 1–4.
[21] G.Z. Voronoi, Recherches sur les paralléloèdres primitives, J. Reine Angew. Math. 134 (1908) 198–287.
[22] P.M. Larsen, S. Schmidt, J. Schiotz, Robus structrual identification via polyhedral template matching, Model. Simul. Mater. Sci. Eng. 24 (2016) 055007.
[23] A. Stukowski, Visualization and analysis of atomistic simulation data with OVITO - the open visualization tool, Model. Simul. Mater. Sci. Eng. 18 (2010) 015012.
[24] S. Plimpton, Fast parallel algorithms for short-range molecular dynamics, J. Comput. Phys. 117 (1995) 1–19.
[25] Y. Mishin, D. Farkas, M.J. Mehl, D.A. Papaconstantopoulos, Interatomic potentials for monoatomic metals from experimental data and ab initio calculations, Phys. Rev. B 59 (1999) 3393–3406.
[26] L.P. Davila, V.J. Leppert, E.M. Bringa, The mechanical behavior and nanostructure of silica nanowires via simulations, Scr. Mater. 60 (2009) 843–846.
[27] J. Diao, K. Gall, M. Dunn, Yield strength asymmetry in metal nanowires, Nano Lett. 4 (2004) 1863–1867.
[28] W. Xu, L.P. Davila, Size dependence of elastic mechanical properties of nanocrystalline aluminum, Mater. Sci. Eng. A 692 (2017) 90–94.
[29] A. Froseth, H. Van Swygenhoven, P.M. Derlet, The influence of twins on the mechanical properties of nc-Al, Acta Mater. 52 (2004) 2259–2268.
[30] A.H. Chokshi, A. Rosen, J. Karch, H. Gleiter, On the validity of the Hall-Petch relationship in nanocrysalline materials, Scr. Metall. 23 (1989) 1679–1684.
[31] R.W. Armstrong, Hall-Petch description of nanocrystalline Cu, Ni and Al strength levels and strain rate sensitivities, Philos. Mag. 96 (2016) 3097–3108.